Check for updates

Organic Solar Cell with an Active Area > 1 cm^2 Achieving 15.8% Certified Efficiency using Optimized VIS-NIR Antireflection Coating

*Jared Faisst, Ershuai Jiang, Shankar Bogati, Leonie Pap, Birger Zimmermann, Tom Kroyer, Uli Würfel, and Mathias List**

Organic solar cells are on the verge of reaching 20% power conversion efficiency (PCE) on small device areas (< 0.1 cm^2). Herein, an improved efficiency of organic solar cells based on the donor polymer D18 combined with the non-fullerene acceptor Y6 with an active area of ≥1 cm^2 reaching a certified PCE of 15.8% is reported. This is achieved due to an increase in photogenerated current enabled by a fully magnetron sputtered multilayer antireflection coating (ARC) custom designed for the absorption profile of the photoactive layer. The influence of this ARC in the visible to near infrared range is quantified by means of full optical device simulations predicting a photogenerated current gain of 3.9%. With the advanced device architecture, the best solar cell is measured independently by Fraunhofer ISE calibration lab obtaining the following values: open-circuit voltage = 851.3 mV, short-circuit current density = 25.11 mA cm^{-2}, fill factor = 73.89% on an active area of 1.0645 cm^2 thus yielding the improved world record efficiency in the category of cell areas ≥1 cm^2.

1. Introduction

With the drastically increasing need for clean and sustainable energy sources worldwide, the photovoltaic (PV) technology has emerged as a major cornerstone addressing this demand. One of the fast-growing research fields in PV technology today are organic solar cells. A major step ahead for the field of organic PV was the introduction of non-fullerene acceptors (NFA) enabling the organic solar cell to harvest the red and near-infrared (NIR) part of the spectrum.[1–4] Namely, the NFA Y6 used in this study has enabled record breaking efficiencies as first synthesized and reported by Zhou et al. (for convenience, the short names are used for the photoactive materials. The long chemical names can be found in the Supporting Information).[5] Combined with the donor polymer D18, as also used in this study, efficiencies of 18% and beyond have been achieved.[6–8] Zhu et al. have reported the – to date– highest certified efficiency of 19.2% using a combination of the donor polymers D18 and PM6 together with the acceptor L8-BO, a modified version of the Y6 NFA.[9,10] Similar to this current record, which was achieved on an active area of 0.052 cm^2, most other published high performance organic solar cells are also constructed on comparably small active areas.[10–12] Serving as repositories, both the National Renewable Energy Laboratory (NREL) chart[13] and the solar cell efficiency table[14] document the progression of certified solar cell record efficiencies achieved under AM 1.5G illumination. While the NREL chart does not pose any restrictions on the active area, the solar cell efficiency table does require a minimum size of 1 cm^2, though it also lists smaller devices as "notable exceptions". Regarding the category of organic solar cells with active areas >1 cm^2, the currently listed certified record efficiency is 15.24% as published in our previous work.[14,15] We were now able to improve on this value by reducing the reflection of incident light at the surface of the solar cell (glass) using an antireflection coating (ARC). Reflection losses can be reduced by multiple methods such as implementing layers that provide a gradual transition of the refractive index from air to glass leading to reduced Fresnel reflection.[16] Another option is to introduce high and low refractive index dielectric layers, which make use of destructive interference for the reflected light to selectively enhance transmission in a certain energy band, known as multilayer dielectric mirror.[17,18] Depending on the design, an ARC can be used to not only increase the transmitted light which incidences perpendicularly but also to enhance transmission specifically from lower angles by implementing microstructures onto the glass surface.[19,20] In this work, we present a custom VIS-NIR multilayer dielectric ARC for solar cells illuminated through the glass substrate based

J. Faisst, E. Jiang, S. Bogati, L. Pap, B. Zimmermann, T. Kroyer, U. Würfel, M. List
Organic and Perovskite Photovoltaics
Fraunhofer Institute for Solar Energy Systems ISE
Heidenhofstr. 2, 79110 Freiburg, Germany
E-mail: mathias.list@ise.fraunhofer.de

E. Jiang, U. Würfel
Freiburg Materials Research Center FMF
University of Freiburg
Stefan-Meier-Str. 21, 79104 Freiburg, Germany

The ORCID identification number(s) for the author(s) of this article can be found under https://doi.org/10.1002/solr.202300663.

© 2023 The Authors. Solar RRL published by Wiley-VCH GmbH. This is an open access article under the terms of the Creative Commons Attribution License, which permits use, distribution and reproduction in any medium, provided the original work is properly cited.

DOI: 10.1002/solr.202300663

on the principles of the dielectric mirror using silicon dioxide, silicon nitride, and titanium dioxide. This ARC is manufactured by magnetron sputtering and thus can easily be upscaled to large areas. The superior performance of the introduced ARC is shown in a comparison to other common antireflective coatings.

2. Results and Discussion

The power conversion efficiency (PCE) of the solar cell is given by the key parameters short-circuit current density (J_{SC}), open-circuit voltage (V_{OC}), fill factor (FF), and power of incident illumination (P_{in}).

$$\mathrm{PCE} = \frac{J_{SC} V_{OC} \mathrm{FF}}{P_{in}} \tag{1}$$

The PCE can be raised by increasing the portion of incident light absorbed by the photoactive layer that translates into an increase in J_{SC}. The organic solar cells presented in this study are illuminated through the glass substrate. This architecture suffers from an undesirable reflection at the surface of the substrate due to the difference of refractive indices of air and glass. To reduce the loss from unintentional reflection, a carefully designed dielectric multilayer ARC is applied to the illumination side of the glass substrate. The full layer stack of the organic solar cell with the multilayer ARC comprising silicon dioxide, silicon nitride, and titanium dioxide is given in **Figure 1**a. For detailed device fabrication of the organic solar cell, see "Device fabrication" in the Methods section.

Figure 1b depicts the simulated absorption of the D18:Y6 layer (red line) within the given organic solar cell stack. Note, that the calculation of this absorption profile only considers light that enters the glass substrate and is therefore independent of the reflection at the air/glass or air/ARC/glass interface (see 'Optical modeling' in the methods section for details).

Based on the absorption profile of the photoactive layer and considering that a multilayer dielectric ARC only enhances transmission in a limited wavelength range, the ARC is optimized for maximum transmission in the wavelength range between 400 and 900 nm as indicated in yellow in Figure 1b. The upper wavelength boundary is chosen to benefit from the high photon flux densities in the NIR range of the illumination spectrum (AM1.5G). Next, the thicknesses of all layers of the ARC were varied through optical simulations to ensure maximum transmission (this optimization using custom code is described under "Simulation and optimization of the antireflection coating" in the Methods section). The optimized ARC consists of 97 nm SiO_2, 148 nm Si_3N_4, 40 nm SiO_2, and 8.5 nm TiO_2, and the transmission of the ARC-coated glass is depicted in Figure 1b. For comparison, the transmission of the uncoated glass substrate is depicted. Figure 1c depicts the simulated and measured reflection of the glass substrate with ARC together with the measured reflectance of the bare glass for comparison. The measured reflectance of the antireflection-coated glass matches the simulation quite well, which demonstrates good accordance of the deposited layers thicknesses with the targeted values. Note that the shown reflections contain the reflection of the glass/air interface at the backside of the substrate, which will not be present in the full device stack.

In the following, optical simulations are used to calculate the photogenerated current gain with the custom designed ARC. The transmission of light into the substrate ($T_{air/substrate}$) for bare glass and glass with ARC are plotted in **Figure 2**a (left axis). The solar irradiance in air ($I_{AM1.5G,air}$) and the irradiance transmitted into the glass substrate ($I_{AM1.5G,substrate}$) with and without ARC are added (right axis). The latter were calculated using:

$$I_{AM1.5G,substrate} = I_{AM1.5G,air} T_{air/substrate} \tag{2}$$

The spectral response (SR) of the solar cell is calculated by

$$\mathrm{SR} = \frac{ehc}{\lambda} I_{AM1.5G,air} T_{air/substrate} A_{D18:Y6} \mathrm{IQE} \tag{3}$$

using the absorption of the D18:Y6 layer ($A_{D18:Y6}$), the internal quantum efficiency (IQE) of the solar cell, the wavelength λ and the product ehc of elementary charge, Planck's constant, and the speed of light. The calculated SR is plotted in Figure 2b assuming an ideal IQE of 1, which represents the upper limit for current generation. The ideal photogenerated current densities J_{PG}, given by the integral of the SR over wavelength, are calculated as 25.7 mA cm^{-2} on bare glass and 26.7 mA cm^{-2} on glass with ARC. This yields a relative increase of 3.9%. A comparison of the experimentally obtained J_{SC} under AM1.5G (corrected for spectral mismatch) of devices with and

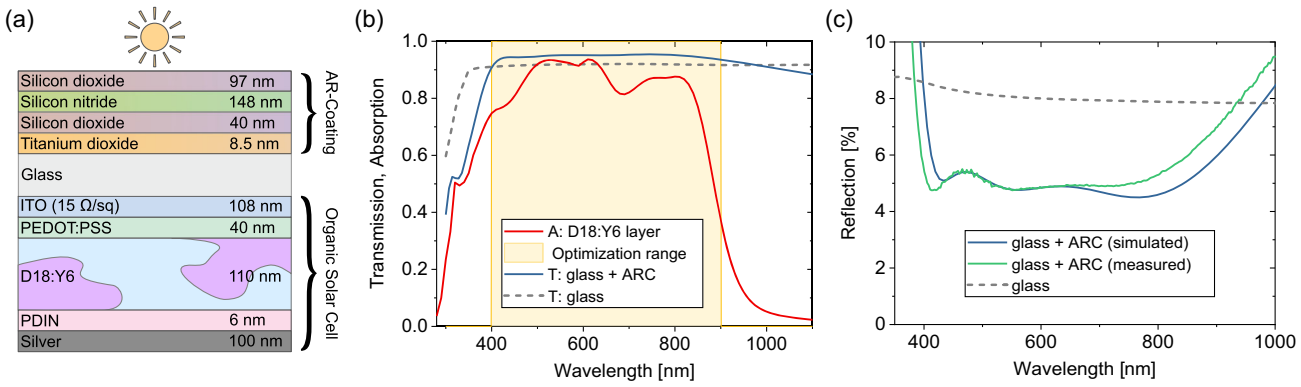

Figure 1. a) Designed ARC stack and the organic solar cell architecture, b) the corresponding transmission of the glass substrate with and without the custom ARC, and c) simulated and measured reflection of the glass substrate.

© 2023 The Authors. Solar RRL published by Wiley-VCH GmbH

2367198x, 0, Downloaded from https://onlinelibrary.wiley.com/doi/10.1002/solr.202300663 by Fraunhofer Ise Inst. Solar Energy Systems, Wiley Online Library on [26/10/2023]. See the Terms and Conditions (https://onlinelibrary.wiley.com/terms-and-conditions) on Wiley Online Library for rules of use; OA articles are governed by the applicable Creative Commons License

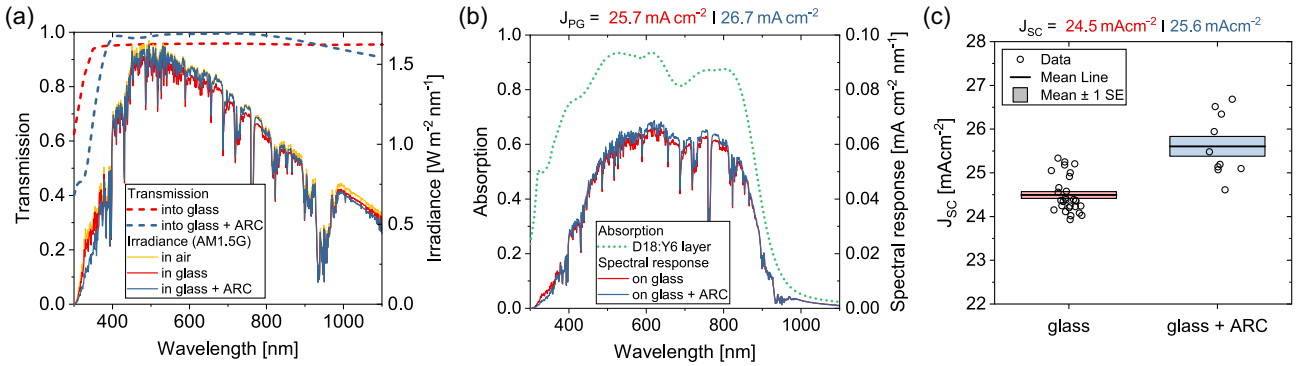

Figure 2. a) Transmission of light into the substrate of the solar cell (dashed lines, left axis) with and without ARC and the irradiance in air and inside the substrate (solid lines, right axis). b) Calculated absorption of the D18:Y6 absorber layer within the full stack (dashed line, left axis) and calculated ideal SR (solid lines, right axis) and the resulting ideal photogenerated current densities J_{PG}. c) Comparison of the measured J_{SC} of an organic D18:Y6 solar cell with and without ARC.

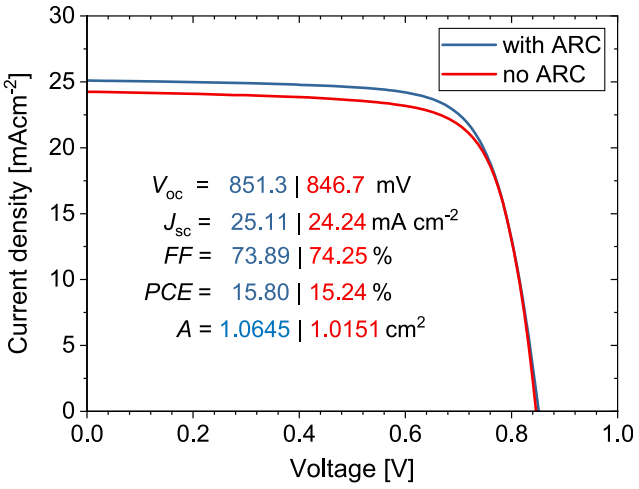

Figure 3. Certified *J–V* curves of D18:Y6 organic solar cells with and without antireflection coating.

without ARC is given in Figure 2c. The mean short circuit current densities are 24.5 and 25.6 mA cm^2, respectively, showing a relative increase of 4.5%. This experimentally observed mean increase agrees with the predicted 3.9% from the calculations within one relative standard error (SE = 0.8%). The absolute numbers are discussed later based on the values from the certified measurements.

The *J–V* curves under illumination (AM 1.5G, corrected for spectral mismatch) measured by *Fraunhofer ISE CalLab PV cells* with the obtained key parameters are given in **Figure 3** for the cell with ARC and the cell on bare glass (published in our previous work).[15] The certified key parameters for the device with ARC are J_{sc} = 25.11 mA cm^{-2}, V_{oc} = 851.3 mV, FF = 73.89% on an active are of 1.0645 cm^2 yielding a world record PCE of 15.80% for organic solar cells >1 cm^2. The certificate can be found in the Supporting Information.

In comparison to the previous record device without ARC, the relative increase in PCE of 3.7% stems mainly from the increase in J_{SC} by 3.6% (24.24–25.11 mA cm^{-2}). For this device, the increase of J_{SC} is in good agreement with the predicted increase of 3.9% calculated earlier.

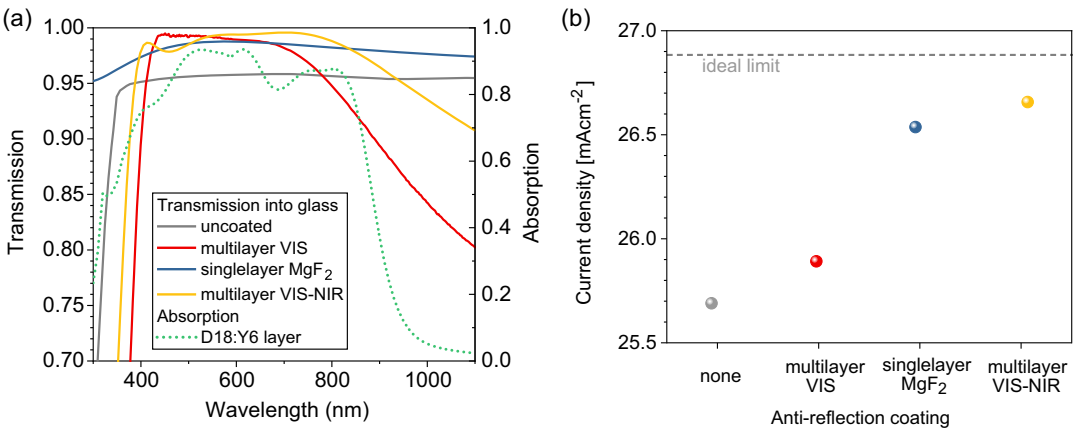

Figure 4. a) Transmission of light into the glass substrate for uncoated, multilayer VIS coated, single-layer MgF_2 coated and multilayer VIS-NIR-coated glass. b) Corresponding calculated photogenerated current densities. The depicted ideal limit is calculated for an ideal transmission (100%) of light into the substrate.

© 2023 The Authors. Solar RRL published by Wiley-VCH GmbH

2367198x, 0, Downloaded from https://onlinelibrary.wiley.com/doi/10.1002/solr.202300663 by Fraunhofer Ise Inst. Solar Energy Systems, Wiley Online Library on [26/10/2023]. See the Terms and Conditions (https://onlinelibrary.wiley.com/terms-and-conditions) on Wiley Online Library for rules of use; OA articles are governed by the applicable Creative Commons License

Comparing the calculated (ideal) photogenerated current density J_{PG} from optical simulations with the certified J_{SC}, we obtain an excellent IQE $= J_{SC}/J_{PG} = 0.94$ with and without ARC. For D18:Y6-based organic solar cells, high IQE of 0.99 have been reported in literature, which is in good agreement (5% deviation) with our work considering experimental uncertainty of the certified J_{SC} of ± 0.35 mAcm^2 and the simulated J_{PG} from uncertainties of the used values (experimentally determined refractive indices, extinction coefficients, and layer thicknesses).[6]

In the following, we compare other applicable ARCs to the coating presented above based on the resulting calculated photogenerated current densities. Therefore, the VIS-NIR ARC is compared to our inhouse dielectric multilayer VIS coating (optimized for 400–700 nm) and to a single-layer MgF_2 ARC with an optimal thickness of 105 nm (for thickness optimization see Supporting Information). The calculated transmissions into the glass substrate are depicted in **Figure 4**a. The corresponding photogenerated current densities plotted in Figure 4b are calculated as described earlier (IQE = 1). The presented optimized VIS-NIR ARC results in the highest photogenerated current lacking only 0.22 mA cm^{-2} compared to the ideal limit calculated for 100% transmission of light into the glass substrate. While a 105 nm single MgF_2 layer ARC also yields promising results (0.34 mA cm^{-2} below the ideal case), the ARC optimized for the visible range only shows minor improvements compared to uncoated glass.

3. Conclusion

To further improve light utilization of organic solar cells, we have designed a custom antireflection coating tailored for the absorption profile of the non-fullerene acceptor based organic absorber D18:Y6. The ARC consists of silicon dioxide, silicon nitride, and titanium dioxide and was fully magnetron sputtered allowing efficient upscaling. The ARC was optically modeled yielding a simulated photogenerated current increase of 3.9% for the D18:Y6 device, which is the highest increase of three different antireflective coatings compared in this work. Therewith, we were able to improve the record PCE for organic solar cells in the category of ≥ 1 cm^2 to the value of 15.80%. Certified measurements reveal the following key parameters: $V_{OC} = 851.3$ mV, $J_{SC} = 25.11$ mA cm^{-2}, and FF = 73.89% on an active area of 1.0645 cm^2. This translates to a relative increase in PCE of 3.7% compared to the previous record PCE in this category.

4. Experimental Section

Device Fabrication: The solar cells were fabricated using the following device stack: 1) Glass/indium tin oxide (ITO, 115 nm)/PEDOT:PSS (40 nm)/D18:Y6 (90 nm)/PDIN (6 nm)/Ag (100 nm)

The ITO glasses (Visiontek Systems LTD, 15 Ohm) were sonicated twice in acetone, twice in isopropanol, and finally in deionized water for 10 min each. The devices for the comparison of the J_{SC} with and without ARC (Figure 2c) have an active area of 0.0925 cm^2. For the device with a photoactive area above 1 cm^2 a support structure for current collecting of Cr (5 nm)/Au (100 nm) was evaporated on top of the ITO on both sides of the active area at a distance of 0.5 cm. This is done to enhance the conductivity of the ITO electrode thus ensuring that the sheet resistance originates (almost) only from the ITO underneath the active layer as the substrate size is rather large (5 cm × 5 cm). Prior to the liquid coatings, the substrates were treated under ultraviolet (UV) ozone for 20 min. PEDOT:PSS (Ai4083 from Heraeus) filtered through a 0.45 µm syringe filter was spin-coated as hole transport layer at 3000 rpm in air for 60 s, and annealed at 130 °C for 10 min after transfer into a nitrogen filled glovebox. Subsequently, the absorber material D18:Y6 (1-Material, used as received; molecular weight (GPC): ≈105 000; PDI ≈ 2.5) in a ratio of 1:1.6 was spin-coated from chloroform solution with a total concentration of 7 mg mL^{-1} at 750 rpm for 30 s. The solution had been stirred overnight at room temperature and at 60 °C for 15 min shortly before use but cooled down to room temperature for coating. The PDIN (1-Material, used as received) electron transport layer was spin-coated from methanol with a concentration of 2 mg mL^{-1} with 0.27 vol% acetic acid (p.a. grade from Sigma Aldrich) stirred over night at room temperature. The layer was spin-coated at 5000 rpm for 30 s. The top electrode was formed by 100 nm of Ag deposited by thermal evaporation in ultra high vacuum ($<10^{-5}$ mbar). Finally, the cells were encapsulated using an adhesive tape (3M 91 022) as preencapsulation plus an overlapping glass using DELO Katiobond LP 655 UV-curing epoxy as seal. The Ar coating was produced by magnetron sputtering at room temperature. The layers were deposited with medium frequency excitation (≈30 kHz) from dual rotatable tube cathodes. For silicon dioxide and silicon nitride, a reactive process with the target material Si:Al (1 wt% Al, 99.9% purity, from Sindlhauser Materials) was used. Titanium dioxide was deposited using a ceramic TiO_2 target with purity 99.8% from GfE coating materials. The deposition parameters of the three dielectric materials are given in **Table 1**. The gas flow is given in sccm (cm^3 at atmospheric pressure per minute).

Simulation and Optimization of the Antireflection coating: The transmission of the ARC layer stack on glass was simulated using the Fraunhofer ISE inhouse tool RAT, which implements the transfer matrix method for plane wave propagation in homogeneous layered media.[21] Inspired by Lemarquis *et. al* and Mazur et al., layer stacks with alternating high (H) and low (L) refractive index were tried out.[17,18] The principal layer set-ups for an antireflection coating on glass is as follows: Air/L/H/L/H/L/.../glass. As L material, SiO_2 was used, while Si_3N_4 and TiO_2 were used as H materials. The used refractive index (n and k) values are given in the section "optical constants." The individual layer thicknesses were optimized using the downhill simplex algorithm as implemented in the scipy.optimize.fmin.[22] The target was to maximize the transmission in the wavelength range between 400 and 900 nm. For the ease of practical implementation, besides maximizing the optical transmission, the goal was set to minimize the number of layers. The lowest number of layers that allowed a good Ar coating to be designed in this wavelength range was four. This resulted in the stack air/SiO_2 97 nm/Si_3N_4 148 nm/SiO_2 40 nm/TiO_2 8.5 nm/glass. This stack had a simulated light transmission from air into the glass of 98.9% in the 400–900 nm range. When the Si_3N_4 was replaced by TiO_2, a similarly good Ar effect can be obtained after optimizing the individual layer thicknesses.

Optical Modeling: The absorption of the photoactive D18:Y6 layer within the layer stack of the organic solar cell was calculated using an implementation of the scattering matrix (S matrix) method based on custom code.[23–26] To only account for light that entered the glass substrate, the half space at the illumination side was modeled as glass. However, a 1.1 mm-thick glass layer was added to the simulation to account for the absorption of the glass substrate (significant in the UV region). The used layer thicknesses are listed under "Device fabrication",

Table 1. Processing parameters for the magnetron sputtered layers of the ARC.

Material	Ar flow [sccm]	Reactive gas flow [sccm]	Power [kW]	Pressure [hPa]
TiO_2	480	O_2:68	30	1.7
SiO_2	500	O_2:365	19	2.1
Si_3N_4	360	N_2:550	15.7	2.1

© 2023 The Authors. Solar RRL published by Wiley-VCH GmbH

2367198x, 0, Downloaded from https://onlinelibrary.wiley.com/doi/10.1002/solr.202300663 by Fraunhofer Ise Inst. Solar Energy Systems, Wiley Online Library on [26/10/2023]. See the Terms and Conditions (https://onlinelibrary.wiley.com/terms-and-conditions) on Wiley Online Library for rules of use; OA articles are governed by the applicable Creative Commons License

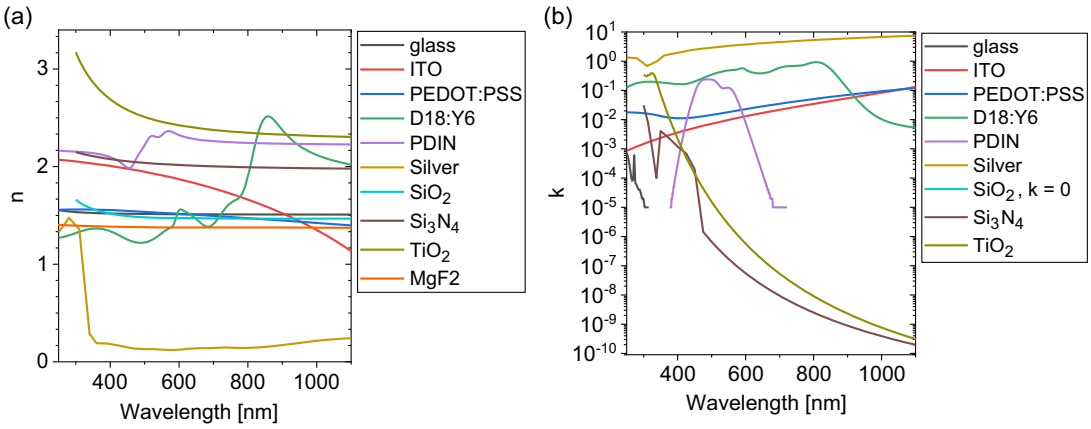

Figure 5. a) Refractive indices and b) extinction coefficients of the used materials. Note that the values of $k = 0$ for glass and PDIN for certain wavelengths cannot be displayed on the logarithmic scale.

the refractive index (n and k) values are given under "optical constants". The presented transmission of light into the glass substrate with and without ARCs was calculated with the same custom code.

Optical Constants: The n and k values of the materials for the organic solar cell were determined from measured reflection–transmission (RT) spectra using PerkinElmer LAMBDA 950 UV/Vis Spectrophotometer equipped with an integrating sphere. The corresponding layer thicknesses were obtained with a Veeco Dektak 150 surface profilometer. The RT spectra were fitted using the software SCOUT from W. Theiss Hard- and Software to determine n and k. The optical data for Ag was taken from literature.[27] The n and k values of the materials used for the ARC (SiO_2, Si_3N_4, and TiO_2) were determined from RT spectra measured with a VERTEX 80 Fourier transform spectrometer by Bruker. The wavelength-dependent refractive indices of these materials were then determined with the Fraunhofer ISE inhouse simulation tool RAT using fits with the Cauchy dispersion model.[28] The obtained values are plotted in **Figure 5**.

Supporting Information

Supporting Information is available from the Wiley Online Library or from the author.

Acknowledgements

The authors acknowledge funding from the German Federal Ministry for Economic Affairs and Climate Protection (FKz. 03EE1119). J.F. acknowledges the scholarship support provided by the German Federal Environmental Foundation (DBU).

Open Access funding enabled and organized by Projekt DEAL.

Conflict of Interest

The authors declare no conflict of interest.

Data Availability Statement

The data that support the findings of this study are available in the supplementary material of this article.

Keywords

antireflection coatings, optical simulations, organic solar cells, record efficiency

Received: August 19, 2023
Revised: September 27, 2023
Published online:

[1] Y. Li, *Acc. Chem. Res.* **2012**, *45*, 723.
[2] Y. Lin, X. Zhan, *Mater. Horiz.* **2014**, *1*, 470.
[3] P. Cheng, G. Li, X. Zhan, Y. Yang, *Nat. Photonics* **2018**, *12*, 131.
[4] A. Armin, W. Li, O. J. Sandberg, Z. Xiao, L. Ding, J. Nelson, D. Neher, K. Vandewal, S. Shoaee, T. Wang, H. Ade, T. Heumüller, C. Brabec, P. Meredith, *Adv. Energy Mater.* **2021**, *11*, 2003570.
[5] R. Zhou, Z. Jiang, C. Yang, J. Yu, J. Feng, M. A. Adil, D. Deng, W. Zou, J. Zhang, K. Lu, W. Ma, F. Gao, Z. Wei, *Nat. Commun.* **2019**, *10*, 5393.
[6] Q. Liu, Y. Jiang, K. Jin, J. Qin, J. Xu, W. Li, J. Xiong, J. Liu, Z. Xiao, K. Sun, S. Yang, X. Zhang, L. Ding, *Sci. Bull.* **2020**, *65*, 272.
[7] K. Jin, Z. Xiao, L. Ding, *J. Semicond.* **2021**, *42*, 60502.
[8] J. Wang, Y. Wang, P. Bi, Z. Chen, J. Qiao, J. Li, W. Wang, Z. Zheng, S. Zhang, X. Hao, J. Hou, *Adv. Mater.* **2023**, *35*, 2301583.
[9] L. Zhu, M. Zhang, J. Xu, C. Li, J. Yan, G. Zhou, W. Zhong, T. Hao, J. Song, X. Xue, Z. Zhou, R. Zeng, H. Zhu, C.-C. Chen, R. C. I. MacKenzie, Y. Zou, J. Nelson, Y. Zhang, Y. Sun, F. Liu, *Nat. Mater.* **2022**, *21*, 656.
[10] Y. Gao, X. Yang, W. Wang, R. Sun, J. Cui, Y. Fu, K. Li, M. Zhang, C. Liu, H. Zhu, X. Lu, J. Min, *Adv. Mater.* **2023**, *35*, 2300531.
[11] R. Sun, W. Wang, H. Yu, Z. Chen, X. Xia, H. Shen, J. Guo, M. Shi, Y. Zheng, Y. Wu, W. Yang, T. Wang, Q. Wu, Y. Yang, X. Lu, J. Xia, C. J. Brabec, H. Yan, Y. Li, J. Min, *Joule* **2021**, *5*, 1548.
[12] J. Yuan, Y. Zhang, L. Zhou, G. Zhang, H.-L. Yip, T.-K. Lau, X. Lu, C. Zhu, H. Peng, P. A. Johnson, M. Leclerc, Y. Cao, J. Ulanski, Y. Li, Y. Zou, *Joule* **2019**, *3*, 1140.
[13] NREL Best Research-Cell Efficiency Chart, https://www.nrel.gov/pv/cell-efficiency.html (accessed: August 2023).
[14] M. A. Green, E. D. Dunlop, M. Yoshita, N. Kopidakis, K. Bothe, G. Siefer, X. Hao, *Prog. Photovoltaics Res. Appl.* **2023**, *31*, 651.
[15] U. Würfel, J. Herterich, M. List, J. Faisst, M. F. M. Bhuyian, H.-F. Schleiermacher, K. T. Knupfer, B. Zimmermann, *Sol. RRL* **2021**, *5*, 2000802.

© 2023 The Authors. Solar RRL published by Wiley-VCH GmbH

2367198x, 0, Downloaded from https://onlinelibrary.wiley.com/doi/10.1002/solr.202300663 by Fraunhofer Ise Inst. Solar Energy Systems, Wiley Online Library on [26/10/2023]. See the Terms and Conditions (https://onlinelibrary.wiley.com/terms-and-conditions) on Wiley Online Library for rules of use; OA articles are governed by the applicable Creative Commons License

[16] K. S. Ram, J. Singh, *Adv. Theor. Simul.* **2020**, *3*, 2000047.
[17] F. Lemarquis, T. Begou, A. Moreau, J. Lumeau, *CEAS Space J.* **2019**, *11*, 567.
[18] M. Mazur, D. Wojcieszak, J. Domaradzki, D. Kaczmarek, S. Song, F. Placido, *Opto-Electron. Rev.* **2013**, *21*, 233.
[19] K. Forberich, G. Dennler, M. C. Scharber, K. Hingerl, T. Fromherz, C. J. Brabec, *Thin Solid Films* **2008**, *516*, 7167.
[20] W. Zhou, M. Tao, L. Chen, H. Yang, *J. Appl. Phys.* **2007**, *102*, 103105.
[21] P. Virtanen, R. Gommers, T. E. Oliphant, M. Haberland, T. Reddy, D. Cournapeau, E. Burovski, P. Peterson, W. Weckesser, J. Bright, S. J. van der Walt, M. Brett, J. Wilson, K. Jarrod Millman, N. Mayorov, A. R. J. Nelson, E. Jones, R. Kern, E. Larson, C. J. Carey, I. Polat, Y. Feng, E. W. Moore, J. VanderPlas, D. Laxalde, J. Perktold, R. Cimrman, I. Henriksen, E. A. Quintero, C. R. Harris, et al., *Nat. Methods* **2020**, *17*, 261.
[22] *SciPy 1.0: Fundamental Algorithms for Scientific Computing in Python* **2020**.
[23] M. List, T. Sarkar, P. Perkhun, J. Ackermann, C. Luo, U. Würfel, *Nat. Commun.* **2018**, *9*, 3631.
[24] Florian Manfred Joachim Bödicker, *Modellierung des strahlenden Emissionsverhaltens in einer photonischen Solarzelle*, Darmstadt **2012**.
[25] L. Li, *J. Opt. Soc. Am. A* **1996**, *13*, 1024.
[26] D. M. Whittaker, I. S. Culshaw, *Phys. Rev. B* **1999**, *60*, 2610.
[27] E. D. Palik, *Handbook of Optical Constants of Solids*, Academic Press, San Diego, CA **2003**.
[28] D. Y. Smith, M. Inokuti, W. Karstens, *J. Phys.: Condens. Matter* **2001**, *13*, 3883.

© 2023 The Authors. Solar RRL published by Wiley-VCH GmbH

2367198x, 0, Downloaded from https://onlinelibrary.wiley.com/doi/10.1002/solr.202300663 by Fraunhofer Ise Inst. Solar Energy Systems, Wiley Online Library on [26/10/2023]. See the Terms and Conditions (https://onlinelibrary.wiley.com/terms-and-conditions) on Wiley Online Library for rules of use; OA articles are governed by the applicable Creative Commons License